Supporting information for

Colloidal Photonic Crystals with Narrow Stopbands Assembled from Low-Adhesive Superhydrophobic Substrates

Yu Huang,[†,‡] Jinming Zhou,[†,‡] Bin Su,[†,‡] Lei Shi,[§] Jingxia Wang,[*,†] Shuoran Chen,[†,‡] Libin Wang,[†,‡] Jian Zi,[§] Yanlin Song,[*,†] and Lei Jiang[†]

[†]Beijing National Laboratory for Molecular Sciences (BNLMS), Laboratory of New Materials, Key Laboratory of Organic Solids, Institute of Chemistry, Chinese Academy of Sciences, Beijing 100190, P. R. China

[‡]Graduate University of Chinese Academy of Sciences, Beijing 100049, P. R. China

[§]Department of Physics and Key Laboratory of Micro and Nano Photonic Structures (Ministry of Education), Fudan University, Shanghai 200433, P. R. China

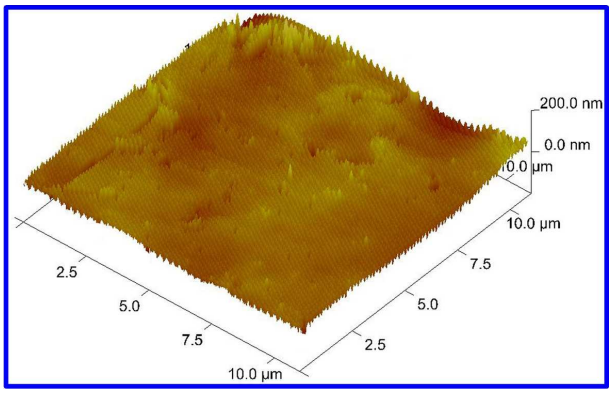

Figure S1. AFM images of as-prepared colloidal PCs with ultra-narrow stopband.

Long-range and well-ordered assembled structure was observed in colloidal PCs assembled from low-adhesive superhydrophobic substrate.

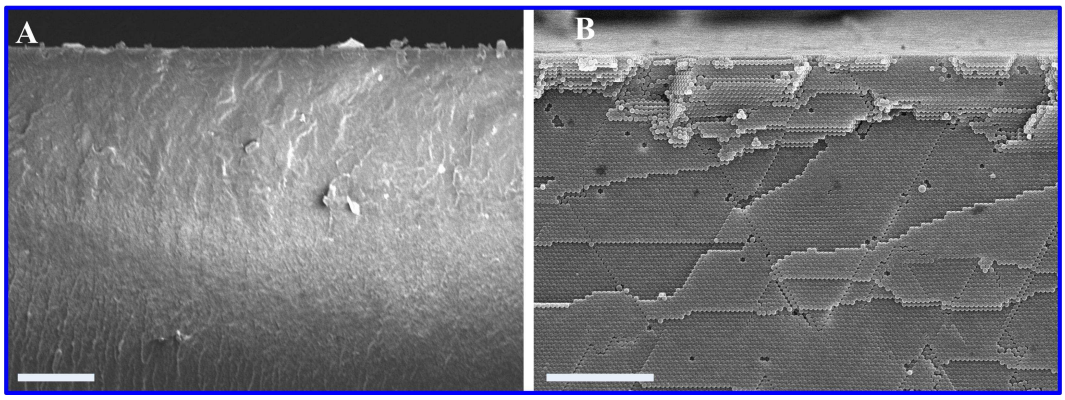

Figure S2. Cross-section SEM images of as-prepared colloidal PCs with ultra-narrow stopband. The scale bar is 100 μm for A and 5 μm for B, respectively.

The SEM images show a well-ordered latex arrangement and sufficient thickness (more than 80 μm) of the as-prepared colloidal PCs.

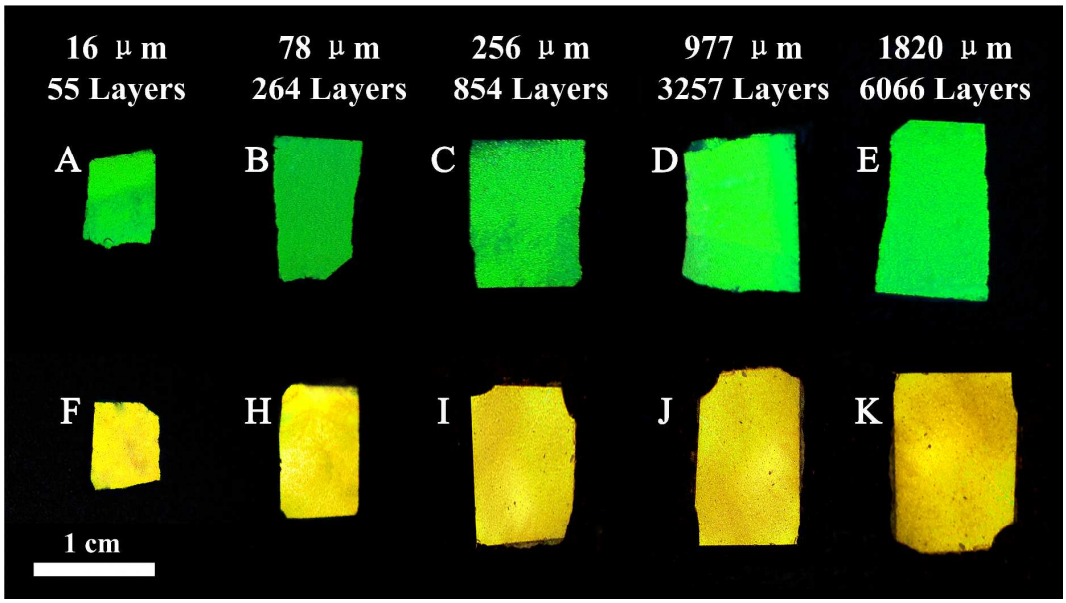

Figure S3. Digital photographs of colloidal PCs with various layers assembled from low-adhesive superhydrophobic substrates. The PCs were assembled from colloidal particles with diameter of 224 ± 3 nm (A-E) and 258 ± 4 nm (F-J): 55 ± 14 layers (A, F), 264 ± 58 layers (B, G), 977 ± 274 layers (C, H), 3257 ± 862 layers (D, I), and 6066 ± 1247 layers (E, J).

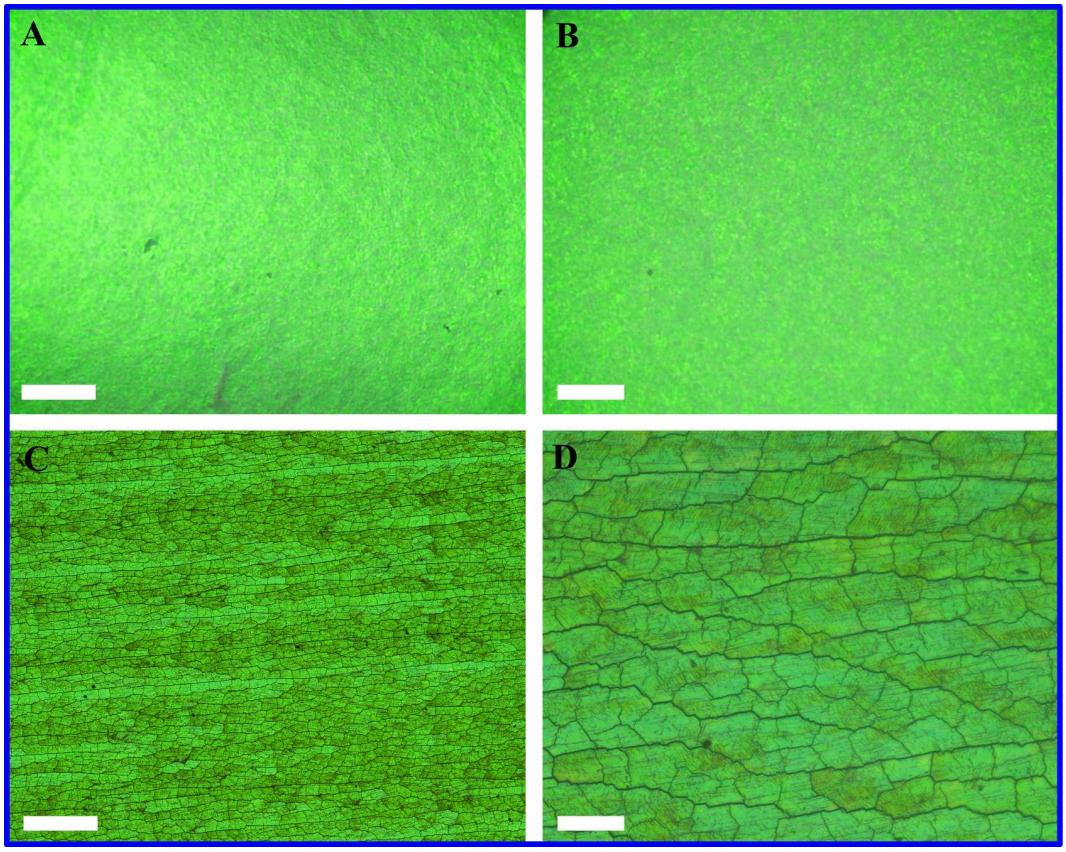

Figure S4. Optical microscope images of colloidal PCs assembled on low-adhesive superhydrophobic (A, B) and high-adhesive substrates (C, D). The scale bar is 100 μm for A, C and 50 μm for B, D, respectively.

The large-scale crack-free PCs (A, B) can be obtained when assembled on low-adhesive superhydrophobic substrates, while the use of high-adhesive substrate results in the formation of the cracked PCs (C, D).

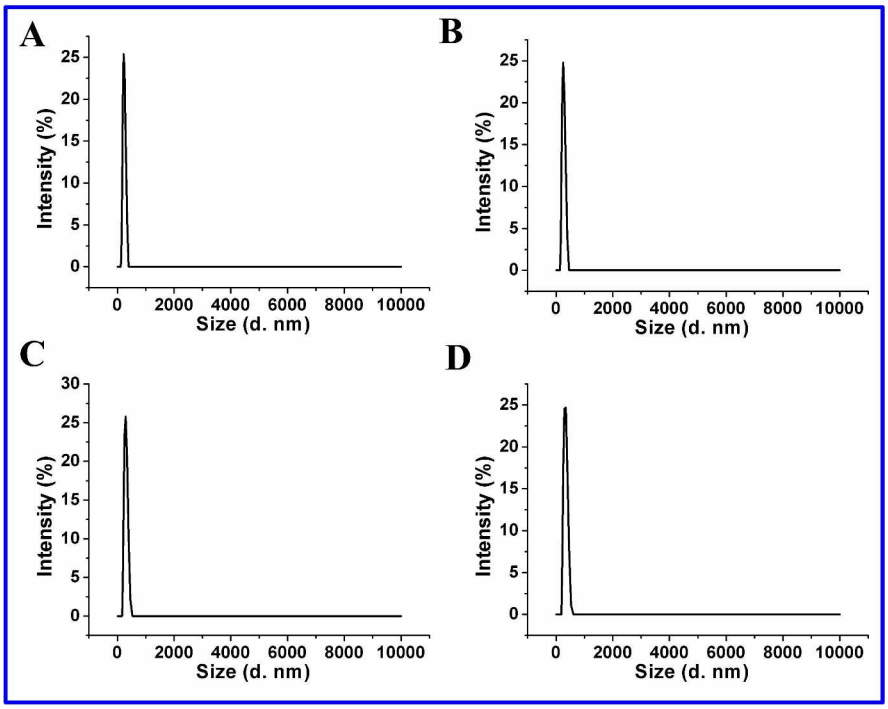

Figure S5. Polydispersity of the latex particles with diameter of 224 nm (A), 258 nm (B), 286 nm (C) and 320 nm (D) obtained by dynamic light scattering (DLS) from Malvern Zetasizer Nano ZS90.

It could be known from the data of Figure S5 that the polydispersity index of as-prepared particles is 0.002, 0.003, 0.006, and 0.002 for the latex particles with diameter of 224, 258, 286 and 320 nm, respectively.

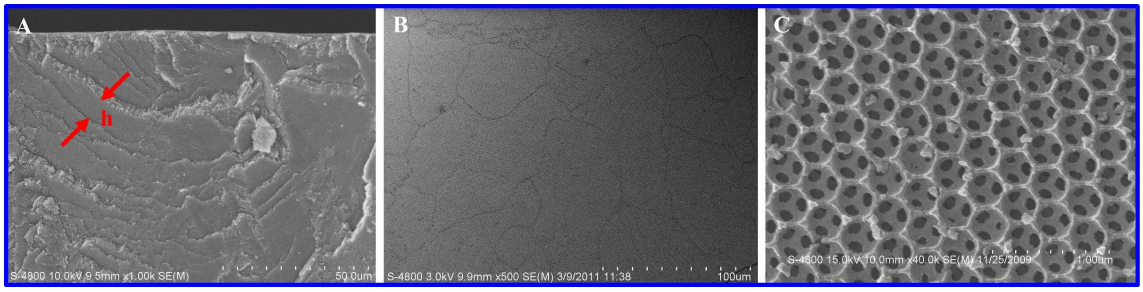

Figure S6. SEM images of as-prepared colloidal PCs: cross-section SEM, demonstrating a minimum thickness of 5 μm, indicated by red arrow (A), top view SEM, displaying the average area of *ca.* 2.78×10^{-9} m^2 for a single domain (B), and relevant inverse opal structure obtained when opal as template, which is used for the calculation of the contact area between particle and substrate. The contact area is *ca*. 1/10 of the whole area (C).

The theoretical critical tensile stress $\boldsymbol{\sigma_c}$ for nucleation of an isolated crack can be deduced from Griffith's energy balance concept:[1]

$$\frac{\sigma_c R}{2\gamma} = 0.1877\left(\frac{2R}{h}\right)^{2/3}\left(\frac{GM\phi_{rcp}R}{2\gamma}\right)^{1/3} \qquad (1)$$

Where, $\boldsymbol{R}$ is the particle radius ($2\boldsymbol{R}$ = 320 nm); γ is the solvent-air surface tension ($\boldsymbol{\gamma}$ = 0.072 N/m); $\boldsymbol{h}$ is the film thickness at cracking; $\boldsymbol{G}$ is the shear modulus of the particles (1.6 GPa); $\boldsymbol{M}$ is the coordination number, and ϕ_{rcp} is the particle volume fraction.

According to the stress-limited regime, the critical thickness is set by the balance of the biaxial stress at the maximum attainable capillary pressure ($\boldsymbol{P_{max}}$) and the critical stress ($\boldsymbol{\sigma_c}$) for cracking, so the critical cracking thickness can be obtained by equating the critical stress ($\boldsymbol{\sigma_c}$) to the tensile stress at the maximum capillary pressure ($\boldsymbol{P_{max}}$):

$$h_{\max} = 0.64\left(\frac{GM\phi_{rcp}R^3}{2\gamma}\right)^{1/2}\left(\frac{2\gamma}{(-P_{\max})R}\right)^{3/2} \qquad (2)$$

$\boldsymbol{h_{max}}$ is the critical thickness under the critical stress for cracking;
Based on the coefficient of the best fit mode of the literature, $\boldsymbol{P_{max}}$ is given by:

$$\frac{(-P_{\max})R}{2\gamma} = 1.4 \qquad (3)$$

So, the equation (2) could be substituted to:

$$h_{\max} = 0.41\left(\frac{GM\phi_{rcp}\,R^3}{2\gamma}\right)^{1/2} \qquad (4)$$

In our experiments, the volume fraction is *ca.* 0.74, $\boldsymbol{M}$ = 6.5, so critical thickness ($\boldsymbol{h_{max}}$) can be calculated, and the value is 5.5 μm, which is closed to the experimental value *ca.* 8 μm (in Figure S6A). Thus, the predicted tensile stress ($\boldsymbol{\sigma_c}$) is 0.562 MPa.

The theoretical critical force (***F***) is the product of theoretical critical tensile stress $\boldsymbol{\sigma_c}$ and contact area (***S***). In this case, the contact area between adjacent layers could be evaluated from the relative inverse opal structure (Figure S6C), and the value is about 3/10 of the whole area. It is known that the latex particles contact the next layer at three-points, but the bottom layer particles contact the substrate at one-point. So, the contact area is about 1/10 of the whole area. As a result, for a single domain with area of *ca.* 2.78×10^{-9} m^2 from average area of single domain in B, the contact area (***S***) is $1/10 \times 2.78 \times 10^{-9}$. The critical force is $\boldsymbol{F} = \boldsymbol{\sigma_c} \times \boldsymbol{S} = 0.562 \times 0.1 \times 2.78 \times 10^{-9} = 156$ μN. The theoretical value of 156 μN, is close to the experimental value F_{ad} of 171 ± 16 μN.

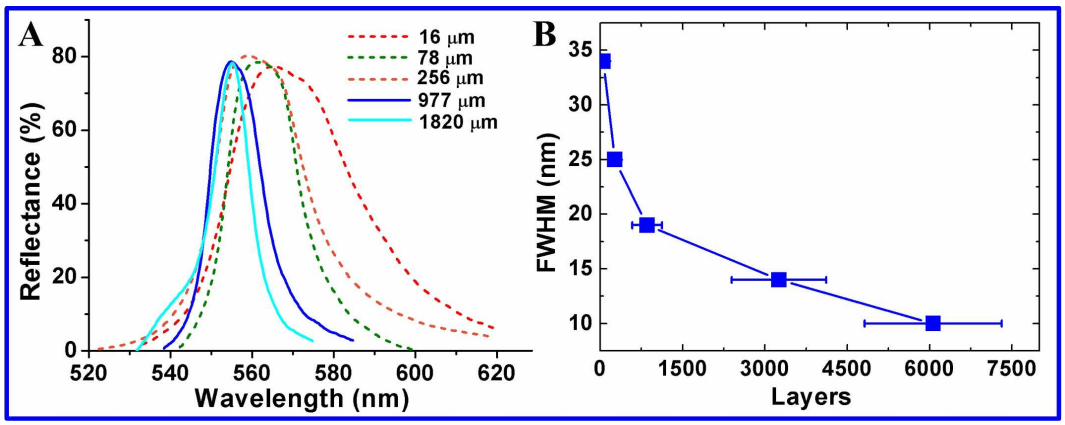

Figure S7. Reflectance spectra of colloidal PCs with diameter of 224 nm (A) and FWHMs with various layers (B) assembled from low-adhesive superhydrophobic substrates.

It could be seen that the FWHMs decrease from 34 to 25, 19, 14, even 10 nm when the layers number of assembled structure grows from 55 ± 14, 264 ± 58, 977 ± 274, 3257 ± 862 to 6066 ± 1247. Figure S7 investigated the relationship of the optic properties with assembly time on low-adhesive superhydrophobic substrate. In this case, when the PCs become thicker, the width of the stopbands become narrower and a blue-shift can be observed. It could be known from the calculated relationship of assembled structure with gap width in Figure 7D, the gap width decrease with ***d/a*** increase (***d***: particle's diameter, ***a***: center-to-center distance between two particles). It means the thick PCs are more close-packed, with less lattice spacing.

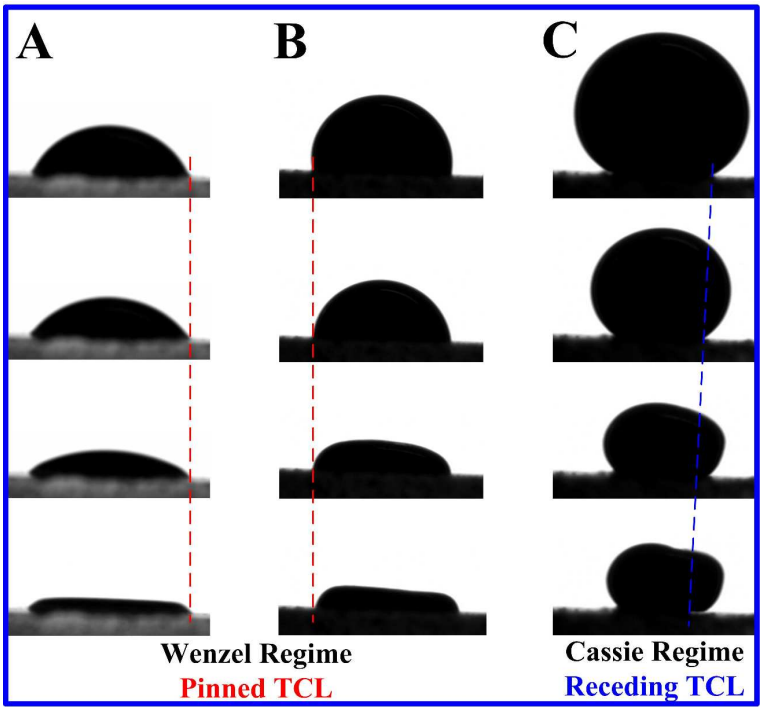

Figure S8. Photographs captured during the latex drop drying process on high-adhesive hydrophilic (A), high-adhesive hydrophobic (B), and low-adhesive superhydrophobic substrates (C). The red dashed line indicates the pinned TCL, and the blue dashed line implies the receding TCL. The phenomenon indicates the different wetting behaviors of the latex drop: Wenzel regime on high-adhesive hydrophilic or hydrophobic substrates and Cassie regime on low-adhesive superhydrophobic substrates.

Different changing modes of three-phase contact line (TCL) are observed during latex droplets drying on three distinct substrates. When the adopted substrate is high-adhesive hydrophilic or high-adhesive hydrophobic substrate (A, B), a stable TCL is found owing to the Wenzel regime of latex droplet. In contrast, a receding TCL is observed on low-adhesive superhydrophobic substrate due to the Cassie wetting behavior of latex droplet (C).

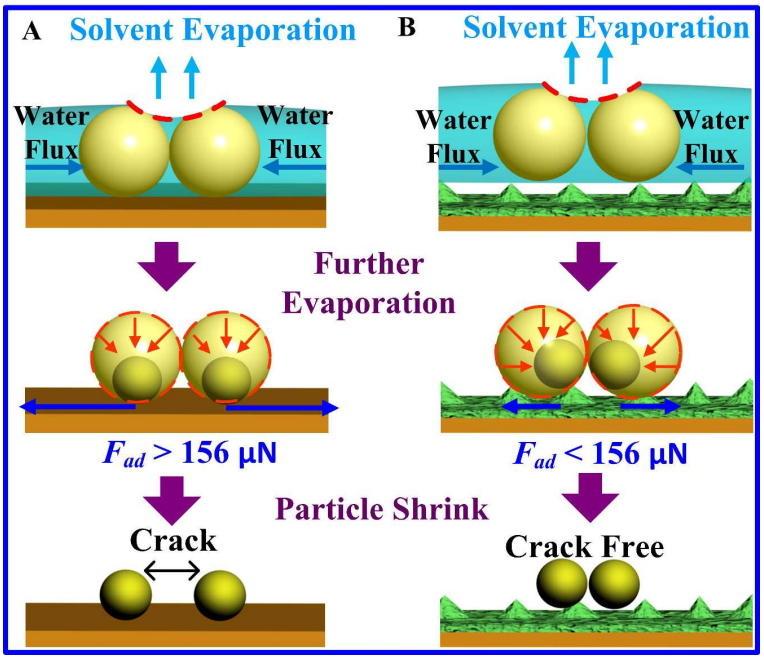

Figure S9. Scheme for the assembly details of latex particles on high-adhesive substrate (A) and low-adhesive superhydrophobic substrate (B).

When latex particles are assembled on a high-adhesive substrate, the F_{ad} limits the latex movement resulting from latex shrinkage, which leads to crack formation. In contrast, latex particles can shrink freely, resulting in a compact latex assembly and complete crack elimination, when the latex particles are assembled on low-adhesive superhydrophobic substrate.

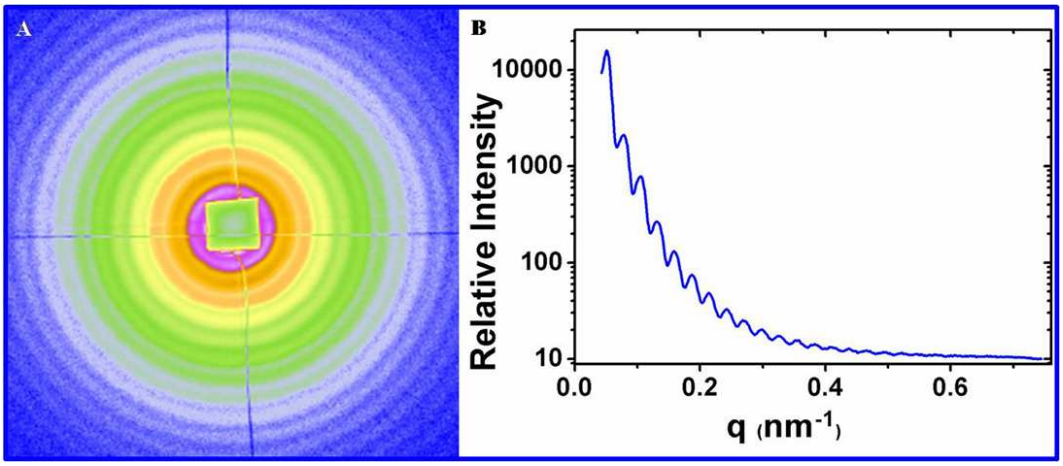

Figure S10. SAXS pattern (A) and relative intensity (B) of PCs assembled on a low-adhesive superhydrophobic substrate using latex particles of diameter 230 nm; q is the effective scattering vector and q_{110} is equal to the medium value of adjacent peaks. In this case, q_{110} is about 0.0269. So the spacing of d_{110} can be obtained form $2\pi/q_{110}$.[2] The calculated value of d_{110} is 233.5 nm, which is very close to the diameter of the latex particles.

The crystal film exhibits typical diffraction features of the Debye-Scherrer ring type, indicating a polycrystalline structure. More than 14 peaks in B and the uniform distances between adjacent peaks imply the high quality of the as-prepared colloidal PCs.

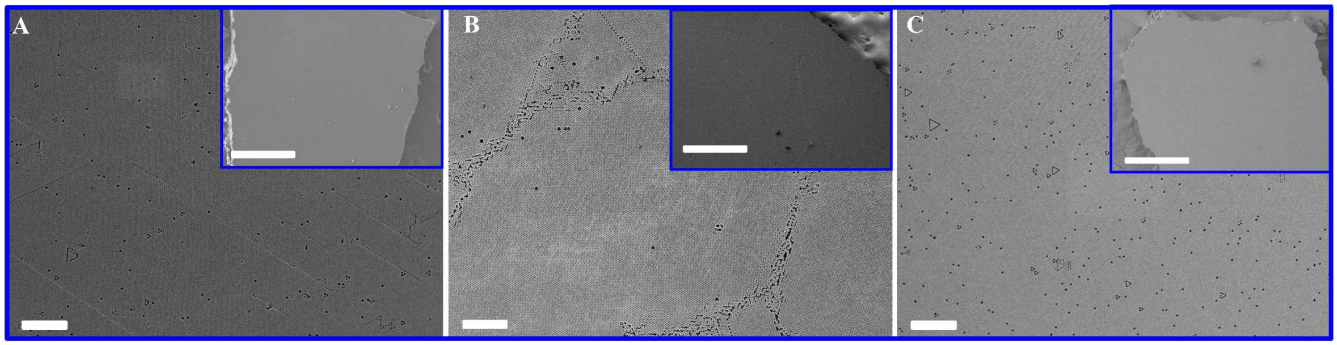

Figure S11. SEM images of colloidal PCs assembled on different low-adhesive superhydrophobic substrates.[3] (A) lotus leaf, (B) TiO_2 substrate with nanovesuvianite structure, and (C) nanoparticle–polymer composite modified substrate. The scale bars are 5 μm, and 0.5 mm for insets.

Large-area crack elimination is observed on colloidal PCs assembled from different low-adhesive superhydrophobic substrates, indicating the universality of this assembly approach.

REFERENCES

(1) Singh, K. B.; Tirumkudulu, M. S. *Phys. Rev. Lett.* **2007**, *98*, 218302.

(2) Duan, L. L.; You, B.; Wu, L. M.; Chen, Min. *J. Colloid. Interf. Sci.* **2011**, *353*, 163.

(3) (a) Feng, L.; Li, S. H.; Li, Y. S.; Li, H. J.; Zhang, L. J.; Zhai, J.; Song, Y. L.; Liu, B. Q.; Lei, J.; Zhu, D. B. *Adv. Mater.* **2002**, *14*, 1857. (b) Lai, Y. K.; Gao, X. F.; Zhuang, H. F.; Huang, J. Y.; Lin, C. J.; Lei, J. *Adv. Mater.* **2009**, *21*, 3799. (c) Cao, L. L.; Jones, A. K.; Sikka, V. K.; Wu, J. Z.; Gao, D. *Langmuir* **2009**, *25*, 12444.